

Supplementary Information

Tailoring particle size of PbI_2 towards efficient perovskite solar cells under ambient air conditions

Qiang Zeng^a, Qingman Ma^a, Linhong Li^{a, b}, Bolin Zheng^c, Yining Pan^a,
Xiangyun Zhao^a, Hanrui Xiao^a, Chang Yan^{c, d, e}, Fangyang Liu^{a, *}

AFFILIATIONS

^a. School of Metallurgy and Environment, Central South University, Changsha 410083, China

^b. Yitai Technology Ltd., Hunan 410083, China

^c. Sustainable Energy and Environment Thrust, The Hong Kong University of Science and Technology (Guangzhou), Nansha, Guangzhou 511400, China

^d. Department of Electronic and Computer Engineering, The Hong Kong University of Science and Technology, Hong Kong SAR, China

^e. Jiangmen Laboratory of Carbon Science and Technology, HKUST(GZ), Jiangmen, China

***Corresponding**

authors:

liufangyang@csu.edu.cn,

Experimental Section

Materials: SnO₂ colloid precursor (tin (iv) oxide, 15% in H₂O colloidal dispersion) was purchased from Alfa Aesar. Dimethylformamide (DMF), dimethyl sulfoxide (DMSO), isopropanol (IPA), chlorobenzene (CB), acetonitrile (ACN), and lithium bis(trifluoromethanesulfonyl)imide (Li-TFSI) were purchased from Sigma-Aldrich. Formamidinium iodide (FAI), methylammonium iodide (MAI), methylammonium chloride (MACl), phenethylammonium iodide (PEAI) and Spiro-OMeTAD (99.8%) were all purchased from Xi'an Polymer Light Technology in China.

For the P-PbI₂ preparation, we followed the method mentioned in our previous report.¹ The excess hydroiodic acid (HI) was added to the clear lead acetate solution with slowly stirring. The clear lead acetate solution was obtained from recycling waste wasted lead acid batteries. Then, the yellow PbI₂ precipitate was obtained immediately. The yellow solid was collected and dried in vacuum at 60°C overnight.

For the PbI₂ crystals (C-PbI₂), a recrystallization process was employed: dissolving P-PbI₂ in hot acetic acid (HAc) aqueous solution with temperature of 80°C and stirring the solution to clear. Then a rapid cooling process to -5°C could promote supersaturation and crystallization of PbI₂, the shimmering golden flake PbI₂ crystals were generated immediately. Following, flake PbI₂ crystals was collected and dried in vacuum at 60°C overnight.

Device Fabrication: ITO glass substrates were sequentially cleaned by detergent, deionized water, and IPA for 15 min, respectively. Then, the ITO glasses were dried by a nitrogen gun and treated with UV-ozone for 20 min. Then the substrate was spin-coated with a thin layer of SnO₂ nanoparticle film (0.5 mL of SnO₂ colloid precursor was diluted in 2 mL of deionized water) at 3,000 r.p.m. for 30 s, and annealed in ambient air at 150 °C for 30 min. The substrates were then treated with UV-ozone for 10 min before deposition of perovskite film. For the fabrication of FAMAPbI₃ perovskite films, a typical two-step sequential deposition method was deployed under different RH conditions. First, 1.5 M of PbI₂ in DMF: DMSO (9:1) solvent was spin-coated onto SnO₂ at 2000 r.p.m. for 30 s, then annealed at 70 °C for 1 min, and then cooled to room temperature. After that, a solution of FAI:MAI:MACl (90 mg: 6.39 mg: 9 mg in 1 ml

IPA) was spin-coated onto the PbI_2 at 2,000 r.p.m. for 30 s, followed by thermal annealing at 150 °C for 15 min. After perovskite formation, the PEAI was dissolved in IPA with concentrations of 5mg/ml and spin-coated onto the perovskite surface at a spin rate of 5,000 r.p.m. for 20s without any further processing. For the hole transporting layer, the solution which consists of 72.3 mg spiro-OMeTAD, 28.8 μL of 4-tert-butyl pyridine, and 17.5 μL of Li-TFSI solution (520 mg of Li-TSFI in 1 mL of ACN) in 1 mL CB, was deposited on perovskite films at 4000 rpm for 20 s. Finally, 70 nm of Ag was thermally evaporated as the electrode under a high vacuum using thermal evaporation system.

Characterization: X-ray diffraction (XRD) measurements were carried out by the PANalytical 2Empyrean 2 with Cu $K\alpha$ radiation ($\lambda=0.15406$ nm, 40 kV, 100 mA). The grazing incidence X-ray diffraction (GIXRD) was determined by using X-ray diffraction analysis (Bruker D8) with a Cu $K\alpha$ radiation source. Inductively coupled plasma (ICP, ICAP7400 Radial) was used to detect impurity element in products. X-ray Photoelectron Spectroscopy (XPS) were carried out by Thermo ESCALAB 250XI. High-resolution scanning electron microscopy (Hitachi Regulus8100) was recorded to observe the grain size of PbI_2 and morphologies for films. The photoluminescence spectra were probed using Edinburgh FLS980. Keithley 2400 source and solar simulator (San-EI Electric) with standard AM 1.5G (100 mW cm^{-2}) illumination were used to perform J-V characteristics. The standard silicon solar cell AK-200 (Konica Minolta) was utilized to calibrate the light intensity. Incident photon to current efficiency (IPCE) spectra was obtained by using QE-R (Enlitech).

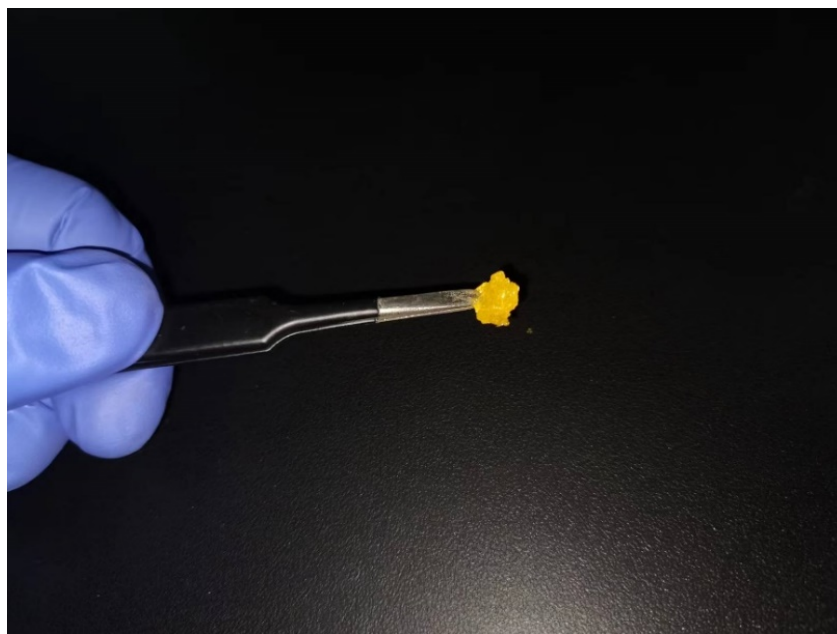


Figure S1 Photograph of centimeter-size C-PbI₂.

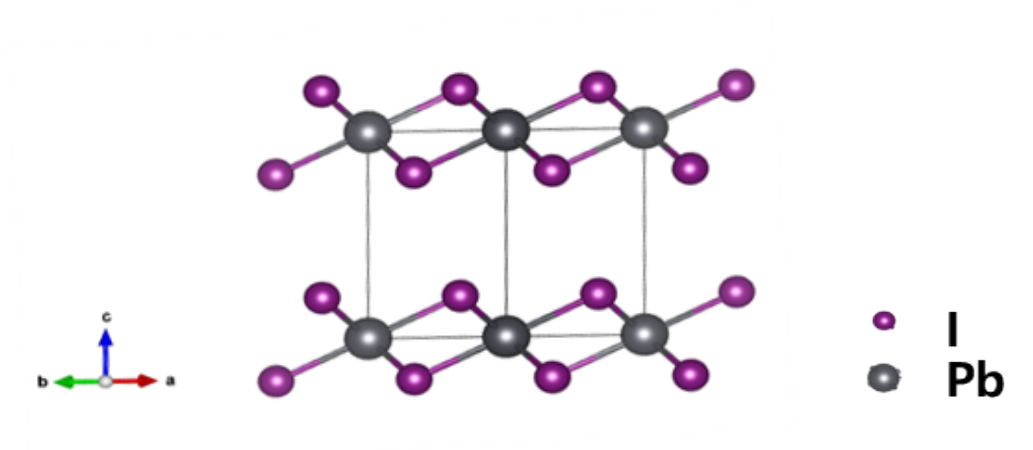


Figure S2 Two-dimensional layer structures of PbI_2

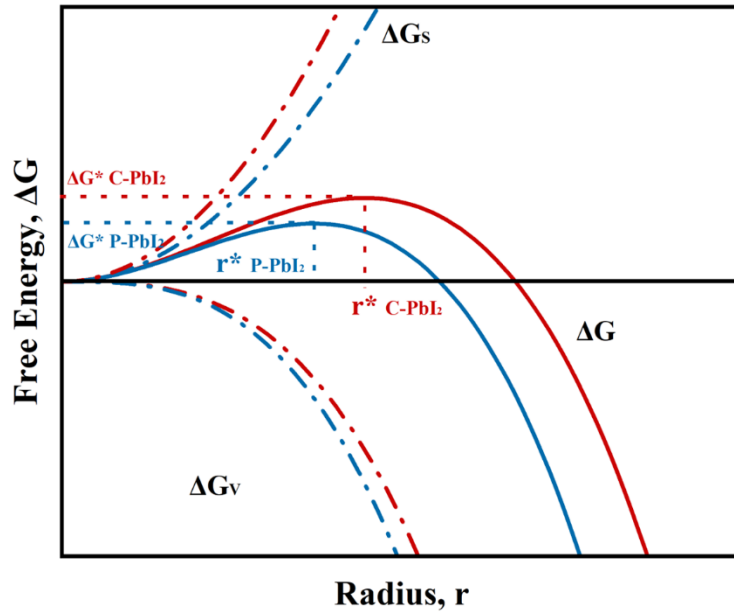


Figure S3 Gibbs free energy change on cluster size based on classical free energy diagram. The processes of nucleation can be considered thermodynamically by examining the total Gibbs free energy (ΔG) defined as the sum of the bulk free energy (ΔG_v) and the surface free energy (ΔG_s), as calculated in equation:

$$\Delta G = \Delta G_v + \Delta G_s = 4\pi r^2 \gamma + \frac{4}{3}\pi r^3 \Delta G_v$$

where r is radius of nucleus and γ is the surface energy. Due to the nucleus is formed from colloid clusters, the radius of nucleus is positive relate to radius PbI_2 cluster. Hence, we plotted the total free energy change of nuclei formation process in figure S5 for P-PbI_2 and C-PbI_2 according to eq 1. Obviously, the P-PbI_2 with small colloid clusters implied slightly free energy (ΔG^*) and critical radius (r^*), which means less nucleation resistance for P-PbI_2 and further crystallization for P-PbI_2 film.

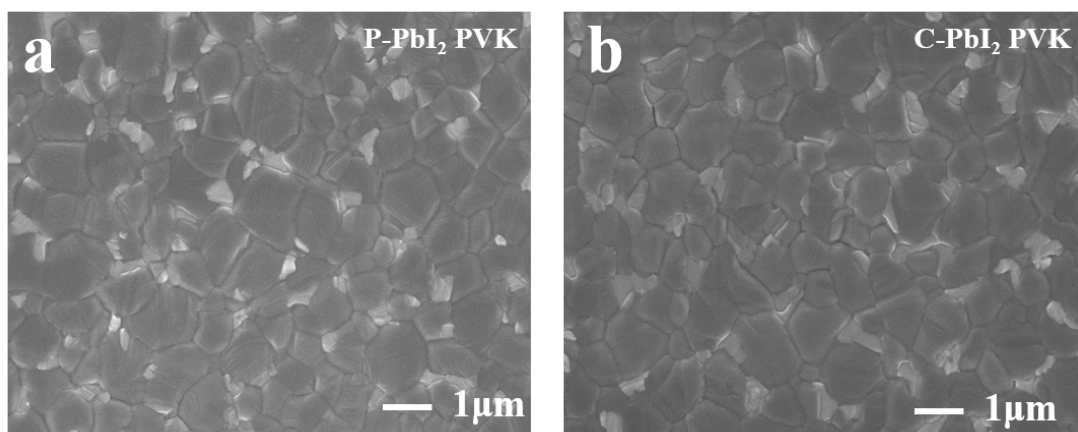


Figure S4 Top-view SEM for a) P-PbI₂ PVK and b) C-PbI₂ PVK films deposited under low RH condition. c) statistical distribution of grain size.

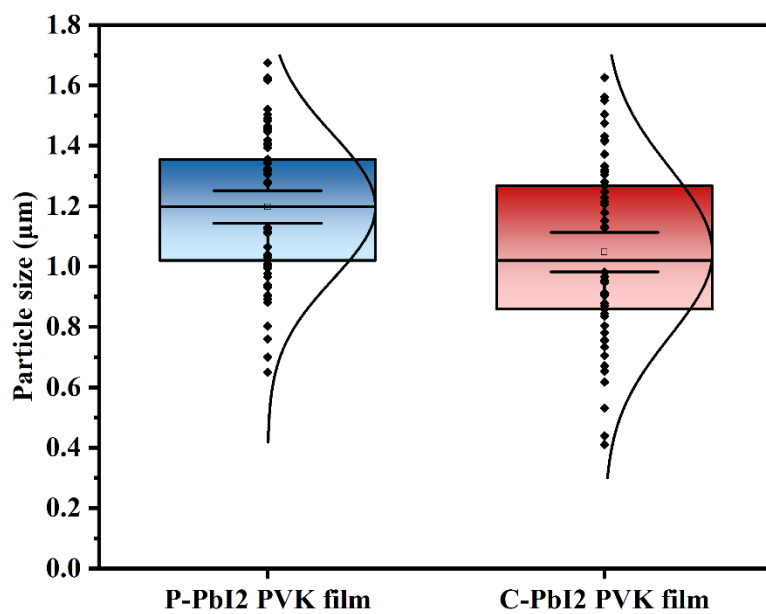


Figure S5 statistical distribution of perovskite grain size.

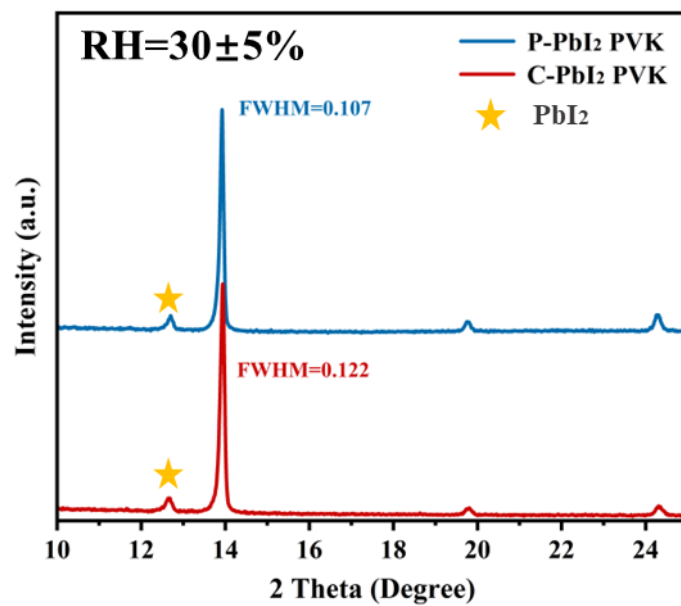


Figure S6 XRD patterns of the P-PbI₂ perovskite and C-PbI₂ perovskite films deposited under low RH=30±5% condition.

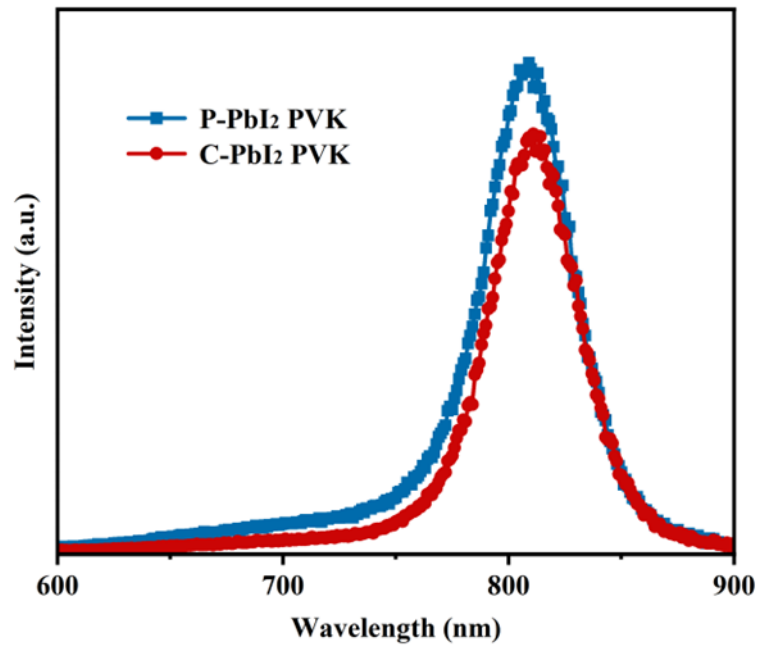


Figure S7 Steady-state PL of the P-PbI₂ perovskite and C-PbI₂ perovskite films deposited on glass substrates under low RH=30±5% condition.

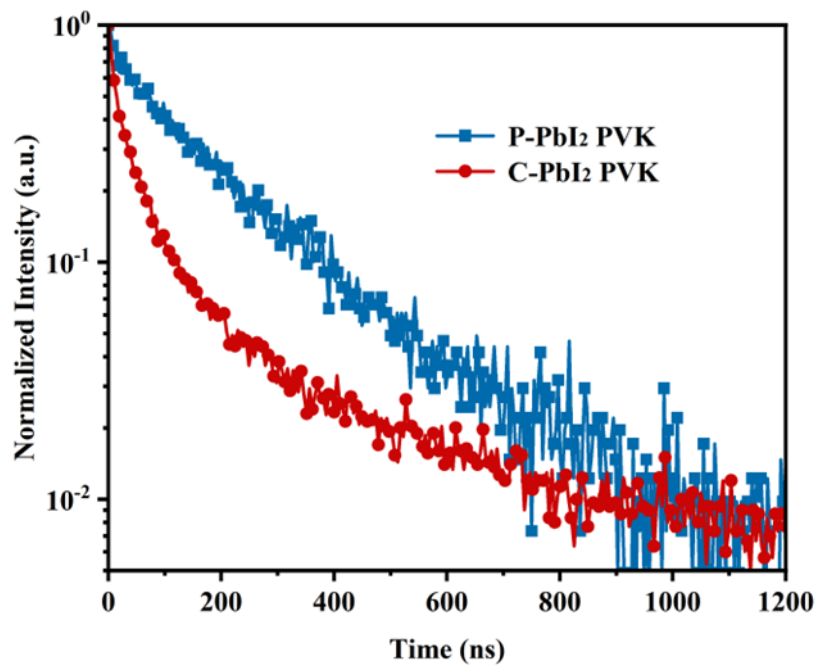


Figure S8 TRPL spectra of the P-PbI₂ perovskite and C-PbI₂ perovskite films deposited on glass substrates under low RH=30±5% condition.

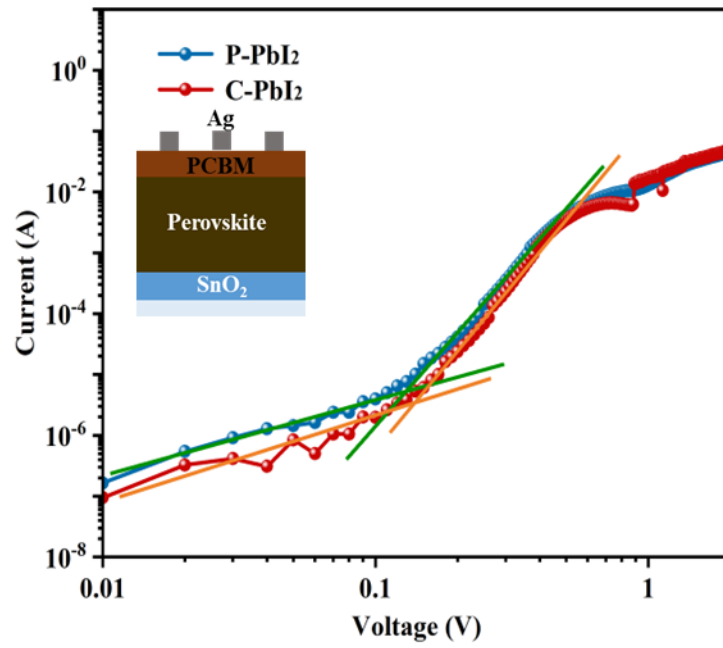


Figure S9 SCLC measurements for the electron-only devices based on P-PbI₂ perovskite and C-PbI₂ perovskite films deposited under low RH=30±5% condition.

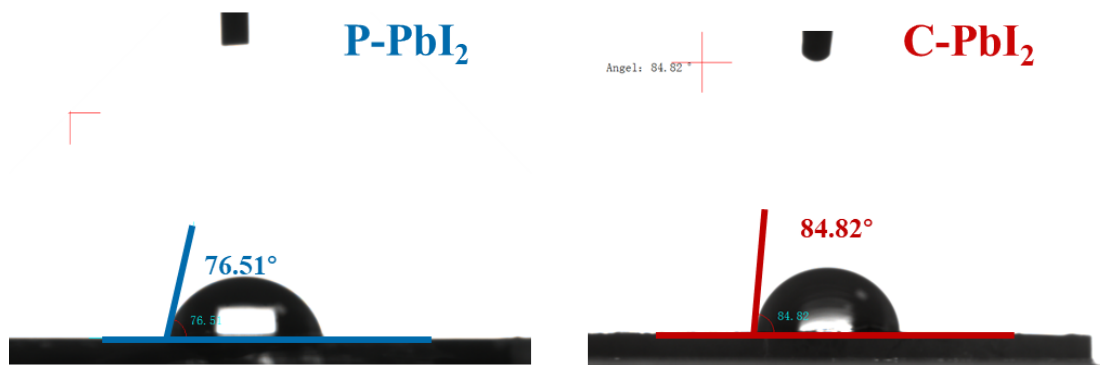


Figure S10 Static contact angles of a water droplet on the surface of PbI₂ wet films

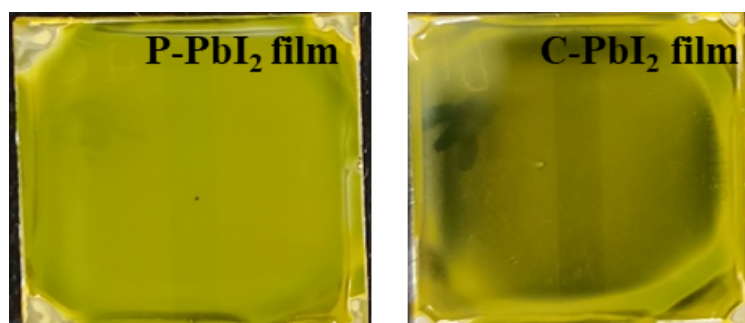


Figure S11 Photograph of P-PbI₂ and C-PbI₂ films deposited under heavy RH=50±5% condition.

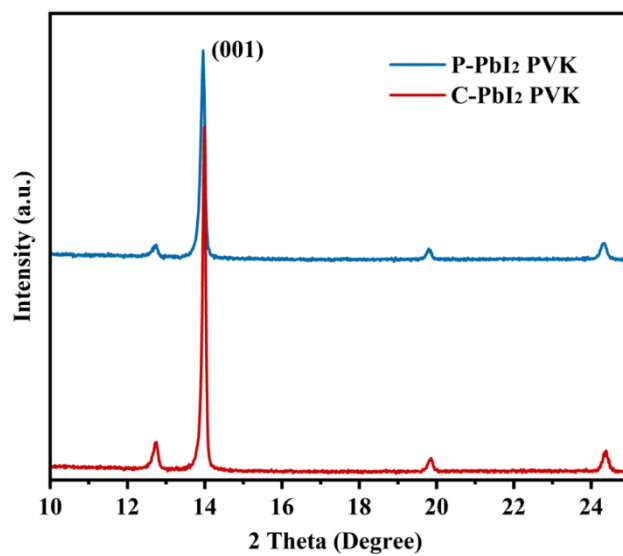


Figure S12 XRD patterns of P-PbI₂ perovskite and C-PbI₂ perovskite films deposited under heavy RH=50±5% condition.

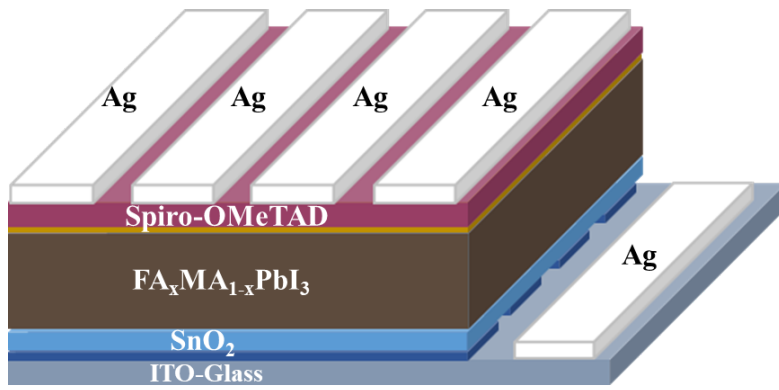


Figure 13 Schematic diagram of the device structure.

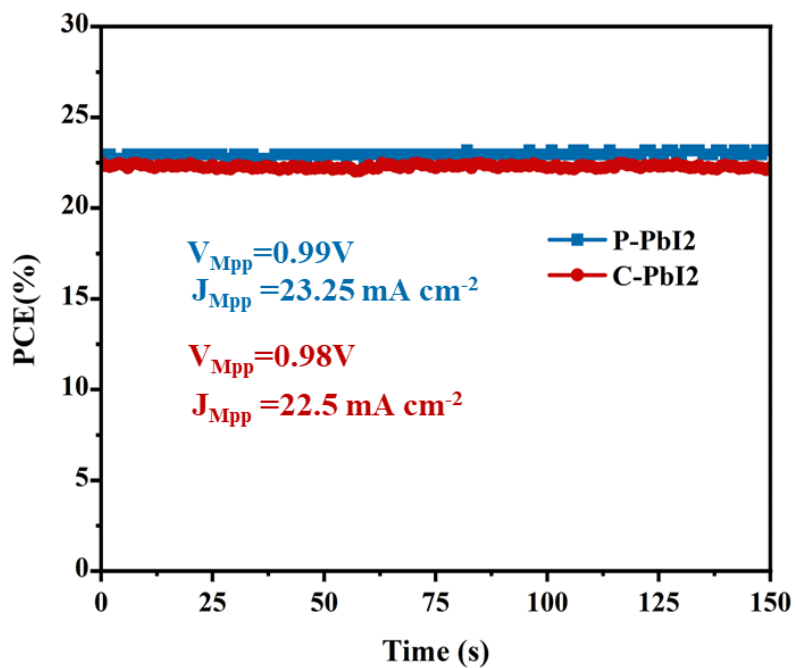


Figure 14 SPO test of the best-performing target devices measured at a constant bias voltage of 0.99 V within 150 s.

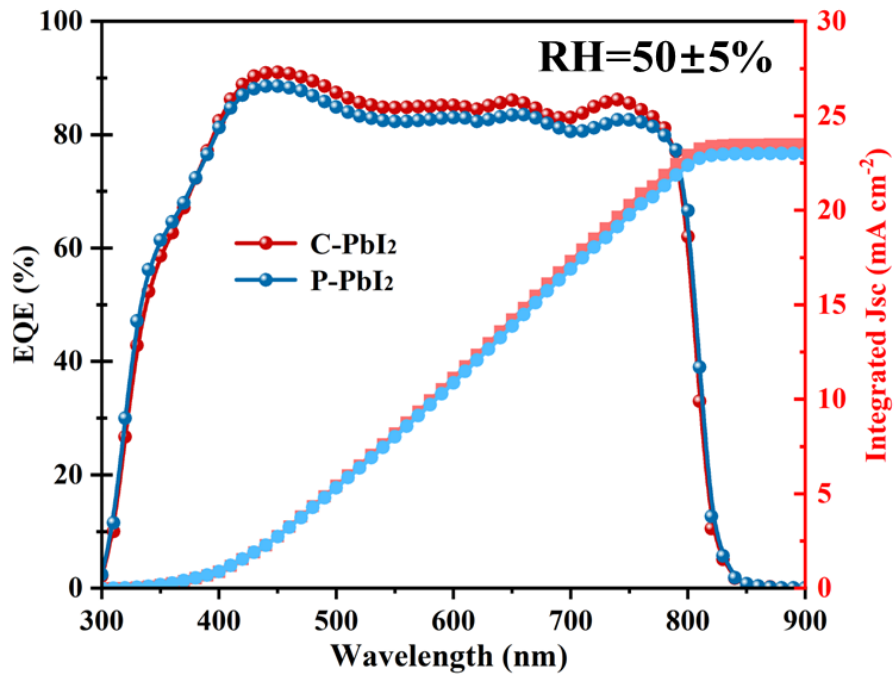


Figure 15 EQE spectra and the corresponding integrated J_{SC} under heavy RH conditions.

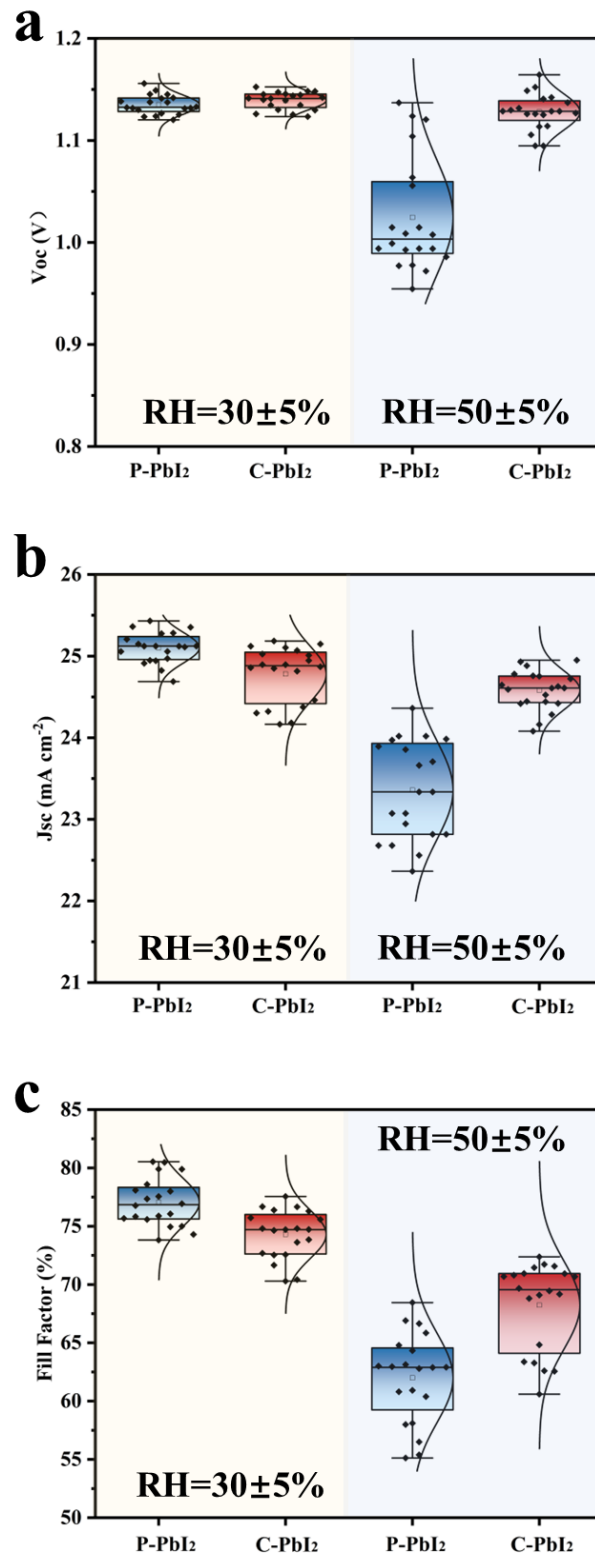


Figure S16 Statistical distributions of the photovoltaic parameters. a) V_{OC} , b) J_{SC} and c) FF.

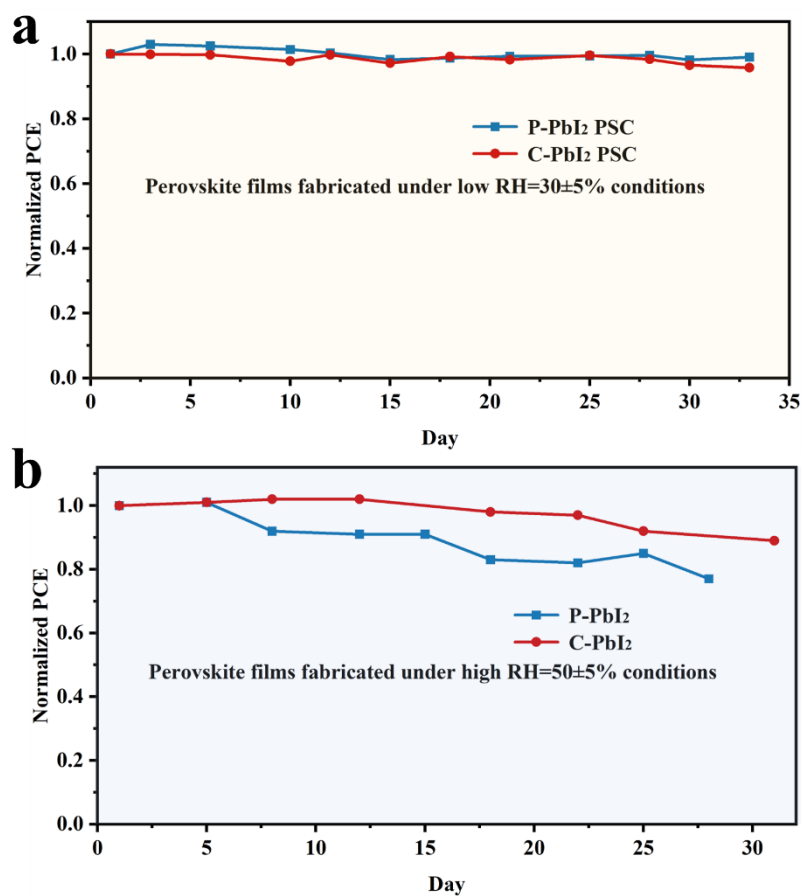


Figure S17 PCE decay of the P-PbI₂ and C-PbI₂ based unencapsulated PSCs stored in an ambient atmosphere (25°C, RH ~ 30%) around 30 days. a. the PVK film were fabricated under low RH condition; b. the PVK film were fabricated under high RH condition.

Table S1 The impurity elements in PbI₂ measured by the ICP.

Elements	Content (ppm)		Elements	Content (ppm)	
	P-PbI ₂	C-PbI ₂		P-PbI ₂	C-PbI ₂
Al	7.6	0.16	Li	/	/
W	/	/	Mg	29.3	0.04
Zn	4.86	/	Mn	/	/
Ba	1.08	/	Mo	/	/
Bi	/	/	Na	17.28	0.28
Ca	18.88	5.05	Ni	/	/
Cd	/	/	Sb	/	/
Co	/	/	Zr	/	/
Cr	0.34	/	Sn	/	/
Cu	/	/	Sr	0.8	/
Fe	1.3	/	Ti	0.74	/
K	11.16	/	V	/	/

Purity: 99.99% for P-PbI₂, 99.999% for C-PbI₂

Table S2 Fitted parameters of the TRPL results.

Prepared conditions	perovskite films	τ_1 (ns)	A_1	τ_2 (ns)	A_2	τ_{ave} (ns)
RH=30±5%	P-PbI ₂	59.225	856.08	442.87	157.94	281.65
	C-PbI ₂	29.126	104.61	200.35	262.08	190.96
RH=50±5%	P-PbI ₂	22.47	772.69	82.12	67.23	36.86
	C-PbI ₂	83.43	806.58	563.81	23.76	163.2
The bi-exponential decay equation:		$I(t) = I_0 + A_1 \exp(-t/\tau_1) + A_2 \exp(-t/\tau_2)$				
The average lifetime (τ_{ave}):		$\tau_{ave} = (A_1\tau_1^2 + A_2\tau_2^2)/(A_1\tau_1 + A_2\tau_2)$				

Table S3 Photovoltaic parameters for best devices.

Relative humidity	Perovskite	V _{OC} (V)	J _{SC} (mA cm ²)	FF (%)	PCE (%)
Low RH=30±5%	P-PbI ₂ Reverse	1.15	25.09	80.73	23.30
	P-PbI ₂ Forward	1.14	25.19	79.24	22.77
	C-PbI ₂ Reverse	1.15	24.82	77.55	22.22
	C-PbI ₂ Forward	1.15	24.94	76.06	21.80
Heavy RH=50±5%	P-PbI ₂	1.13	24.16	66.65	18.31
	C-PbI ₂	1.16	25.00	72.37	21.09

References

1. L. Xie, Q. Zeng, Q. Li, S. Wang, L. Li, Z. Li, F. Liu, X. Hao and F. Hao, *J Phys Chem Lett*, 2021, **12**, 9595-9601.